

Statistics of Chaos

David C. Ni

Dept. of Mathematical Research, Direxion Technology
9F, No. 177-1, Ho-Ping East Rd., Sec 1, Daan District, Taipei, Taiwan, R.O.C.

Abstract. In a previous effort, we demonstrated that transition to chaos being related to symmetry broken of the divergent sets in fractal forms of complex momentum-and-angular-momentum plane, which are constructed by an extended Blaschke product (EBP).

In the recent efforts, we demonstrated root computation via iteration of EBP. Using newly developed algorithms, we iterate the EBP and have mapped the convergent sets in the domains to the disconnected solution sets in the codomains. We demonstrated that solution sets showing various forms of canonical distributions and found counter examples of Fundamental Theorem of Algebra (FTA).

In this paper, we further extend the root-computation algorithms to the transition regions of chaos in the domains and the mapped codomains. We characterize the solution sets and explore the methodologies and the related theories to the modelling of physical phenomena, such as formation of galaxy cluster and stellar system.

Keywords: Nonlinear Lorentz Transformation, Nonlinear Relativity, Blaschke Equation, Fractal, Iterated solutions, Chaos, Statistics, dynamical systems.

1 Introduction

Contemporary models for N-body systems are mainly extended from temporal, two-body, and mass point representation of Newtonian mechanics. Other mainstream models include 2D/3D Ising models constructed from the lattice structures. These models have been encountering on-going debates in statistics. We were motivated to develop a new construction directly from complex-variable N-body systems based on the extended Blaschke functions (EBF)[1], which represent a non-temporal and nonlinear extension of Lorentz transformation on the complex plane – the normalized momentum-angular-momentum space. A point on the complex plane represents a normalized state of momentum and angular momentum (or phase) observed from a reference frame in the context of the theory of special relativity. This nonlinear representation couples momentum and angular momentum through real-imaginary equation of complex number.



The limited convergent sets in the domains and the corresponding codomains demonstrated hierarchical structures and topological transitions depending on parameter space. Among the transitions, continuum-to-discreteness transitions, nonlinear-to-linear transitions, and phase transitions manifest this construction embedded with structural richness for modelling broad categories of physical phenomena. In addition, we have recently developed a set of new algorithms for solving EBF iteratively in the context of dynamical systems. The solution sets generally follow the Fundamental Theorem of Algebra (FTA), however, exceptional cases are also identified. Through iteration, the solution sets show a form of $\sigma + i [-t, t]$, where σ and t are the real numbers, and the $[-t, t]$ shows canonical distributions.

As in the previous paper [2,3,4,5,6,7], we introduce an angular momentum to the EBF, and for the degree of EBF, n , is greater than 2, we observed that the fractal patterns showing lags as shown in Fig. 9(a). As angular momentum increases, the divergent sets (fractal patterns) are connected to the adjacent sets and diffuse as shown in Fig. 9(a). As iteration further increasing, subsequently all convergent sets will become null set, which we define as chaotic state in this paper. The main effort hereby is to extend the solution iteration algorithm to the transition regions, where the domains and codomains becoming chaotic state. Particularly, we characterize the convergent sets in the codomain near the chaotic transition. The related theories and methodologies manifest a new paradigm for modeling chaos. As an example of efforts on the applications of modeling the physical phenomena, we apply the observations to the theories of formation of galaxy clusters and stellar systems.

2 Construction of functions and equations

2.1. Functions and Equations

Given two inertial frames with different momentums, u and v , the observed momentum, u' , from v -frame is as follows:

$$u' = (u - v) / (1 - uv/c^2) \quad (1)$$

We set $c^2 = 1$ and then multiply a phase connection, $\exp(i\psi(u))$, to the normalized complex form of the equation (1) to obtain the following:

$$(u'/u) = \exp(i\psi(u))(1/u)[(u-v)/(1-uv)] \quad (2)$$

We hereby define a generalized complex function as follows:

$$f_{B_i}(z, m) = z^{-1} \Gamma^m C_i \quad (3)$$

And C_i has the following forms:

$$C_i = \exp(g_i(z))[(a_i - z)/(1 - \bar{a}_i z)] \quad (4)$$

Where z is a complex variable representing the momentum u , a_i is a parameter representing momentum v , \bar{a}_i is the complex conjugate of a complex number a_i and m is an integer. The term $g_i(z)$ is a complex function assigned to $\Sigma'2p\pi iz$ with p as an integer. The degree of $f_B(z,m) = P(z)/Q(z)$ is defined as $\text{Max}\{\text{deg } P, \text{deg } Q\}$. The function f_B is called an extended Blaschke function (EBF). The extended Blaschke equation (EBE) is defined as follows:

$$f_B(z,m) - z = 0 \tag{5}$$

2.2. Domains and Codomains

A domain can be the entire complex plane, C_∞ , or a set of complex numbers, such as $z = x+yi$, with $(x^2 + y^2)^{1/2} \leq R$, and R is a real number. For solving the EBF and EBE, a function f will be iterated as:

$$f^n(z) = f \circ f^{n-1}(z), \tag{6}$$

Where n is a positive integer indicating the number of iteration. The function operates on a domain, called domain. The set of $f^n(z)$ is called mapped codomain or simply a codomain. In the figures, the regions in black color represent stable Fatou sets containing the convergent sets of the concerned equations and the white (i.e., blank) regions correspond to Julia sets containing the divergent sets, the complementary sets of Fatou sets on C_∞ in the context of dynamical systems.

2.3. Parameter Space

In order to characterize the domains and codomains, we define a set of parameters called parameter space. The parameter space includes six parameters: 1) z , 2) a , 3) $\exp(gi(z))$, 4) m , 5) *iteration*, and 6) *degree*. In the context of this paper we use the set $\{z, a, \exp(gi(z)), m, \textit{iteration}, \textit{degree}\}$ to represent this parameter space. For example, $\{a\}$, is one of the subsets of the parameter space.

2.4. Domain-Codomain Mapping

On the complex plane, the convergent domains of the EBFs form fractal patterns of with limited-layered structures (i.e., Herman rings), which demonstrate skip-symmetry, symmetry broken, chaos, and degeneracy in conjunction with parameter space [7]. Fig. 1 shows a circle in the domain is mapped to a set of twisted figures in the codomain. We deduce that the mapping related to the tori structures in conjunction with EBFs.

Fig. 2 shows two types of fractal patterns in the domains. These patterns are plots at different scales. In order to demonstrate these figures, we reverse the color tone of Fatou and Julia sets, namely, the black areas are the divergent sets.

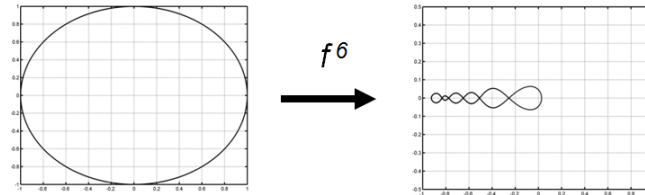


Fig. 1. Domain-Codomain mapping of a unit circle.

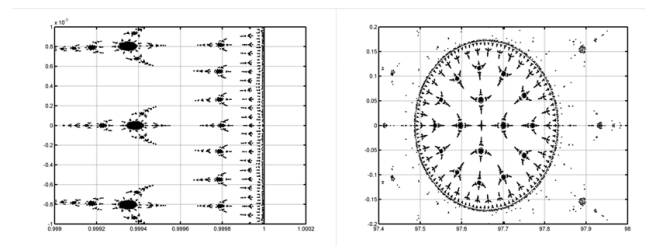


Fig. 2. Fractal Patterns of the divergent sets in the domains.

3 Transitions

3.1. Nonlinear to Linear Transitions

Fig. 3 shows the Fatou sets of domains with different degrees and values of parameter $\{a\}$. Fig. 3 (a) through (d) show that the Fatou sets are quite topologically different for different degrees, from $f_B(z, 1)$, the linear equation to $f_B(z, 4)$. When the value of $\{a\}$ increases from 0.1 to 0.8.

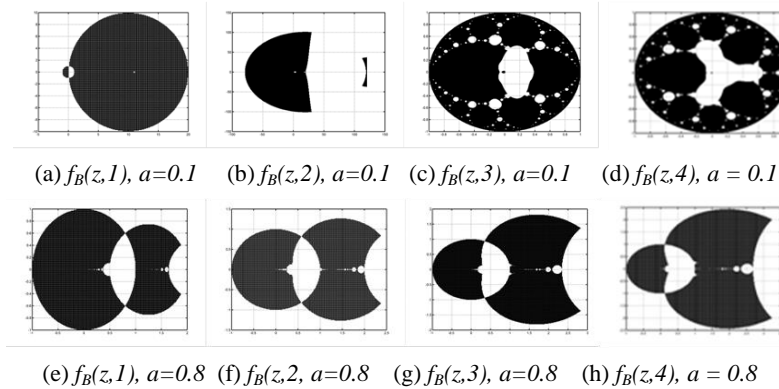


Fig. 3. Convergent sets of $f_B(z, 1), f_B(z, 2), f_B(z, 3),$ and $f_B(z, 4)$ with values of $\{a\}$ at 0.1 and 0.8 respectively.

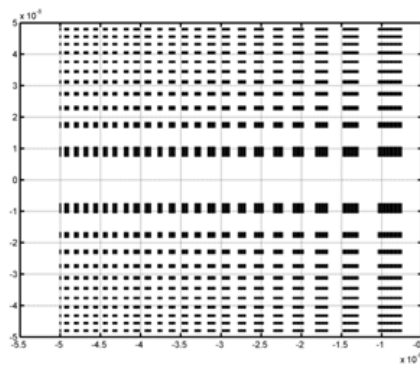
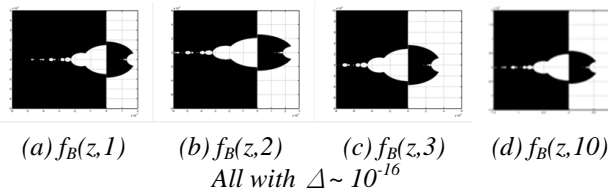
The Fatou sets show topologically similar with minor variations as shown from $f_B(z,1)$, the linear equation to $f_B(z,4)$ or even at higher degrees as in Fig. 3 (e) through (h). We call this phenomenon as nonlinear-to-linear transition.

3.2. Continuum to Discrete Transitions

When the value of $\{a\}$ approaches to unity, the topological patterns of Fatou sets in the domains demonstrate an abrupt or quantum-type transition from the connected sets to the discrete sets. The discrete sets show Cantor-like pattern when mapping onto real axes on the complex plane, nevertheless, these sets are not Cantor sets by definition [6, 7, 8, 9].

The transition of EBF occurs between $a = 1 - 10^{-16}$ and $a = 1 - 10^{-17}$. Fig. 4 shows this type of topological transition. Fig. 4(a) through 4(d) shows the nonlinear-to-linear degeneracy, and 4(e) shows the Cantor-like pattern at all degrees once the transition occurs. Here, we define $\Delta = 1 - a$.

Fig. 5 shows another discreteness-to-continuum transition around a pole in original domains based on the parameter $\{degree\}$. Fig. 6 shows continuum-to-discreteness transitions in mapped domain based on the parameter $\{iteration\}$. These transitions demonstrate a fabric tori structure of EBF.



(e) $f_B(z,m), \Delta = 10^{-17}$

Fig. 4. Connected sets transit to discrete Cantor-like sets for all $f_B(z,m)$ at $\Delta = 10^{-17}$ in the domains.

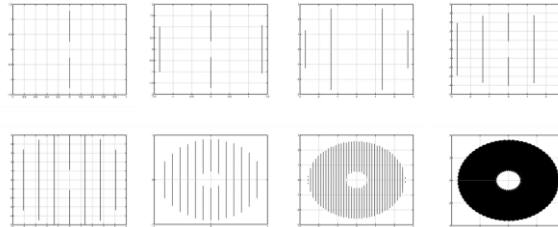


Fig. 5. Discreteness to continuum transitions around a pole of EBF as value $\{degree\}$ increases in the domains.

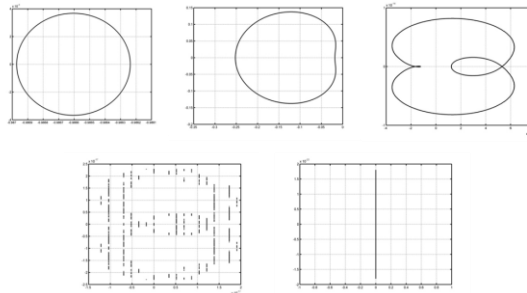


Fig. 6. Continuum to discreteness transitions as value $\{iteration\}$ increases in the domains.

3.3. Topological Transitions

Fig. 7 shows a mapping from the convergent Fatou sets of the domain to the codomain. We examine the plots of three different values: absolute, real, and imaginary on the complex plane. The plots of absolute and real values show a modular pattern with 90 degree rotation. These sets are symmetrical to the y-axis, comparing to the x-axis symmetry of the Fatou sets of the domain. The plots of imaginary values demonstrate conjugate symmetry to the y-axis. Fig. 8 further shows this special feature with different values of $\{a\}$.

Using the color bar (with $z = 0$ at center of the bar) on the right side of individual figures in Fig. 8, we observe the relationship of $z(-x, y) = -z(x, y)$, as so-called conjugate symmetry. From perspective of angular momentum, the indication of this conjugate symmetry is related to the conversation law.

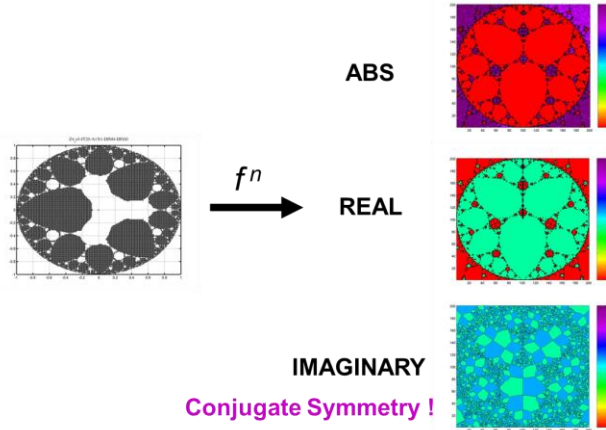


Fig. 7. Separation of Real and Imaginary values in the Domains

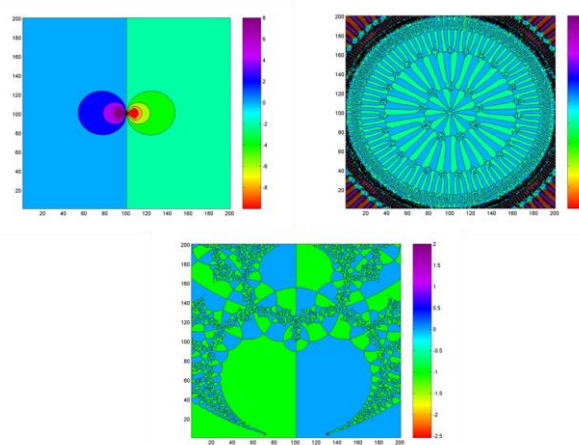


Fig. 8. Three patterns of conjugate symmetry at different values of $\{a\}$.

3.4. Chaotic Transitions

In the following, the convergent sets are colored in blue for those on the upper half of the complex plane, while those sets in red color are on the lower half. By doing so, we are able to examine the mappings in more details.

When an additional angular momentum applied to EBF as equation 7 below:

$$a = 0.1(\cos\theta + \sin\theta) \quad \text{with } degree = 4 \quad (7)$$

In Fig. 9(a), each layer or level of fractals, namely, the divergent sets will be lagged more as the value θ increases, and subsequently connected to the adjacent divergent sets, and eventually diffuse and become null sets for value of $\{degree\}$ is greater than 2 as shown in Fig. 9(a). For value of $\{degree\}$ is 1 or 2, as shown in Fig. 9(b), this type of diffusion will not occur as shown in Fig. 9(b) [3, 4].

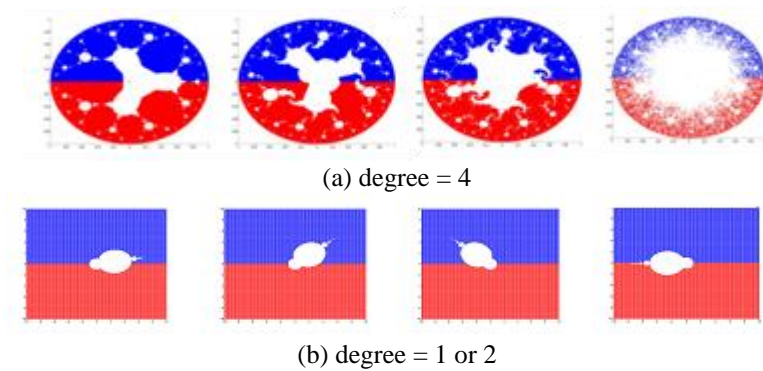


Fig. 9. Additional angular momentum applied to convergent sets

4 EBF Solutions via Iteration

4.1. Solution sets in Domain and Codomain

As shown in Fig. 10, a new set of iteration algorithms are adopted for solving EBFs, and the discrete sets in the codomain demonstrate fixed-point-like solution sets.

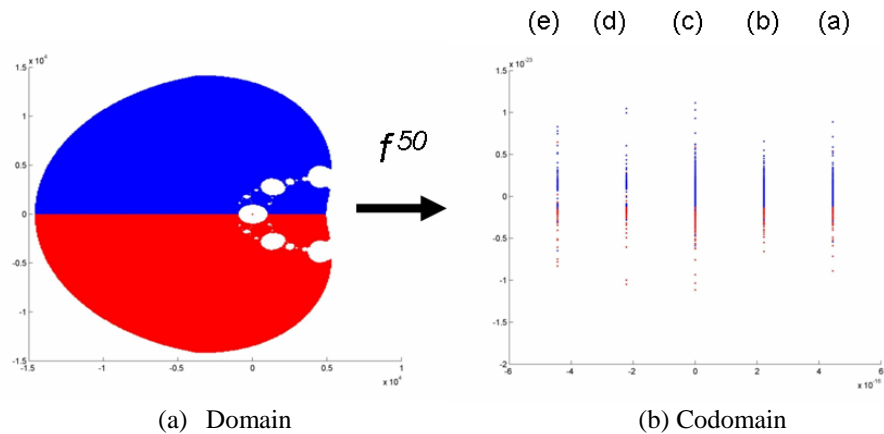


Fig. 10. Iterated sets of EBF for $a = 0.1$ and $degree = 3$ at scale of 10^4 as the domain (10(a)) mapping to the convergent set (a), (b), (c), (d) and (e) in the codomain (10(b)) showing violation of FTA.

As Fundamental Theorem of Algebra (FTA) asserts that the number of solution sets is equal to the degree of EBF, however, we found cases of FTA violation as shown in Fig. 10 [10].

For the individual convergent sets shown in Fig. 10 (b) in the codomain, we can examine closely which sets in the domain are mapping from as shown in Fig. 11. These figures demonstrate a deterministic perspective against the uncertainty of mapping and may fundamentally change the definition of probability in the context of statistics.

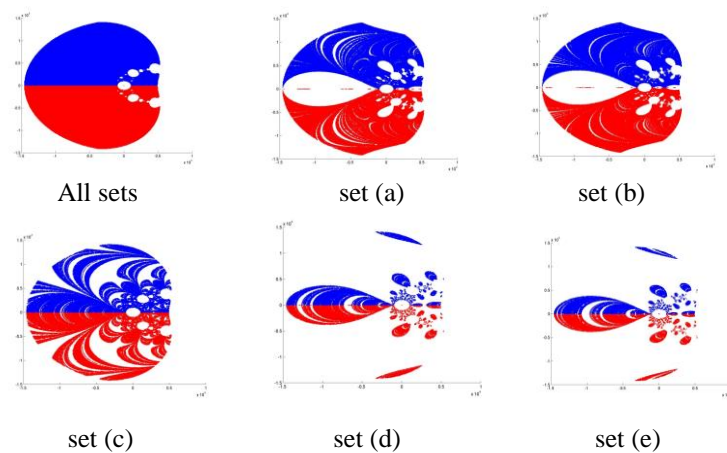


Fig. 11. The individual sets in domain (10(a)) corresponding to the convergent set (a), (b), (c), (d) and (e) in the codomain (10(b)).

Fig. 12 shows solutions by iteration for 7th degree and 12th degree EBFs, the numbers of solution sets are as FTA asserts. The solution sets show that the individual sets with specific real values are with spread-out imaginary sets demonstrating various distributions.

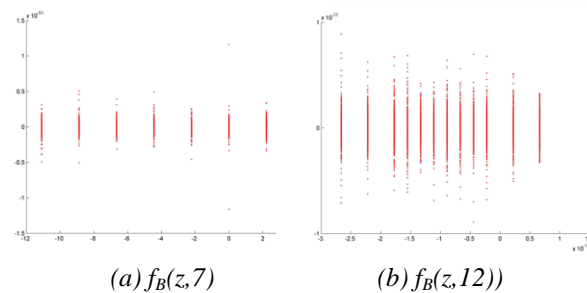


Fig. 12. Two solution plots with two different values of {degree}.

4.2. Distributions

For the individual convergent sets as shown in Fig. 10 (b), we further plot the distributions of real and imaginary point sets with a designated partition as shown in Fig. 13. The plot at bottom of Fig.13 shows the weights of individual sets, while the plot on the right side of Fig. 13 shows overall distribution along the imaginary part, the angular momentum or phase [8, 9].

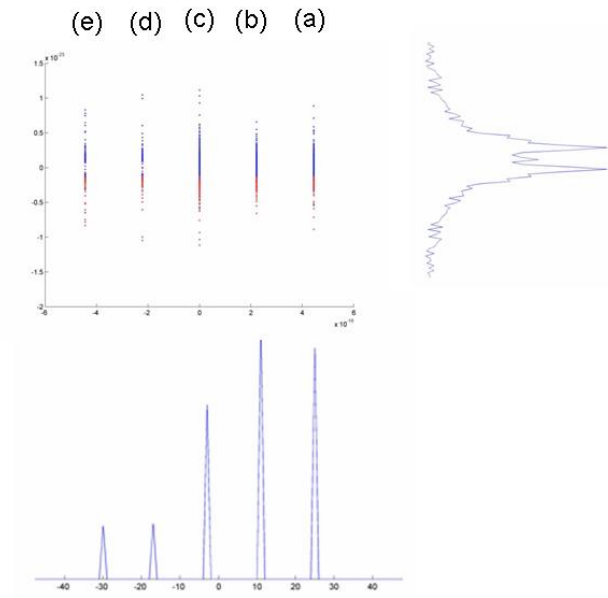


Fig. 13. Distribution plots of convergent sets in the codomain as in Fig. 10(b).

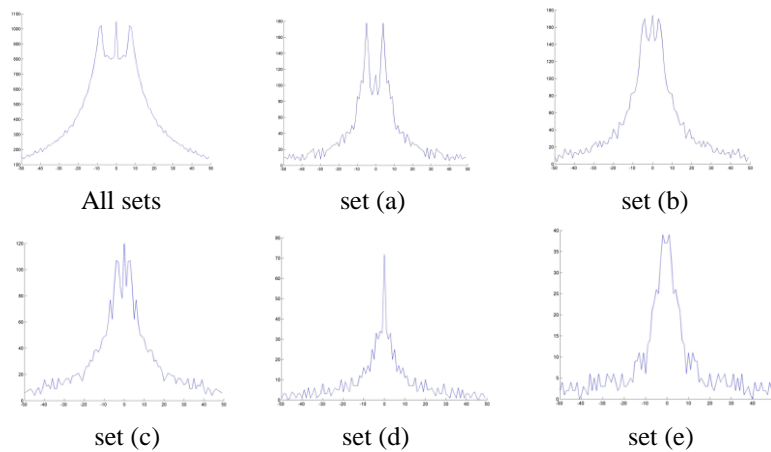


Fig. 14. Distribution plots of individual convergent sets in the codomain.

Further, we plot the distributions of the all and individual sets in Fig. 10 and Fig. 11 as shown Fig. 14. These distributions demonstrate 1-peak, 2-peak, and 3-peak distributions with different peak values. These distributions demonstrate scaling invariant to the parameter $\{iteration\}$.

At different scales of hierarchical convergent sets as same parameter space as in Fig. 10, the convergent sets in codomain demonstrate similar FTA violation, but the distributions are different. Fig. 15 shows that when scale changed from 10^4 to 10^{-4} , the distribution is more a quantum-mechanics distribution as in Fig. 15(b).

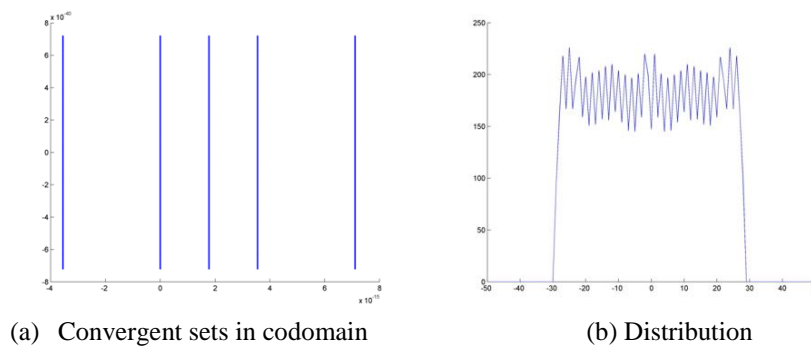


Fig. 15. The convergent sets for $a = 0.1$ and $degree = 3$ at scale of 10^{-4} comparing with that in Fig. 10 and Fig. 13.

5 Pre-Chaos Sets in Domains and Codomains

Applying the methods described in the section 4 to the convergent sets in chaotic transitions described in section 3.4, we can examine closely the convergent sets in the codomains.

5.1. Near the chaotic transitions

As described in equation (7) in section 3.4., we have the following parameters as in equation (8):

$$a = 0.2 (\cos(75*\pi/180) + \sin (75*\pi/180)) \quad \text{with } degree = 3 \quad (8)$$

As the value θ increases and the convergent sets approaching to the chaotic transitions, two divergent sets are both diffusing to the sub-fractal sets and demonstrate a balanced diffusion. Subsequently, the sets converge slowly and present a hierarchical structure of several layers, which are viable for the modelling of observed phenomena in the nature.

Fig. 16 shows the plots the distributions of the convergent sets in the codomain of equation (8).

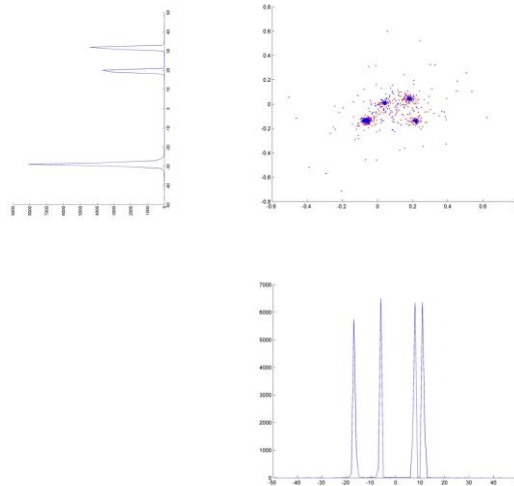


Fig. 16. The distributions of convergent sets for $a = 0.2$, $\theta=(75*\pi/180)$ and $degree = 3$ in the codomain.

Fig. 17 shows three distribution plots corresponding to the imaginary values (left set in Fig. 16) in details. The symmetry showing in Fig. 14 is broken.

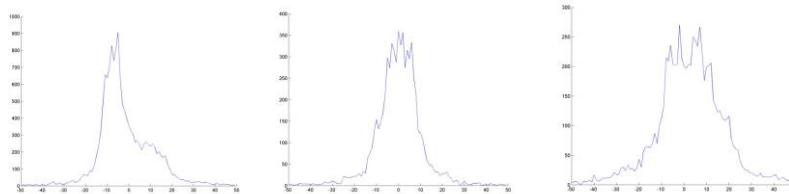


Fig. 17. The distributions of imaginary values of the convergent sets for $a = 0.2$, $\theta=(75*\pi/180)$ and $degree = 3$ in the codomain.

Fig. 18 shows four distribution plots corresponding to real values (bottom set in Fig. 16) in details. Both distribution sets of the real and imaginary values are not symmetrical, nevertheless, they are canonical distributions. The important ideas from these plots for the theoretical constructions are that in the chaotic transitions, the values of momentum and angular momentum are in limited discrete groups. This observation manifests that we can model the turbulence, chaos, and related phenomena more straightforward in momentum-angular-

momentum space than those in temporal space. In the following section, we will further extend this construction based on hierarchical structures.

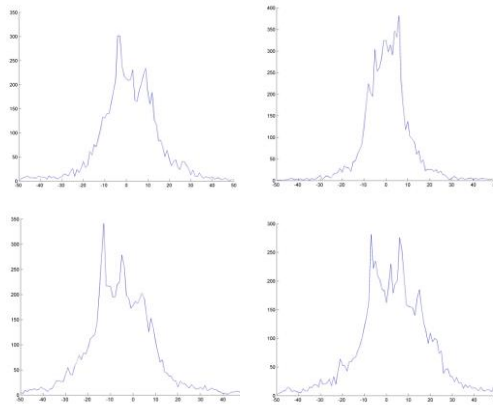


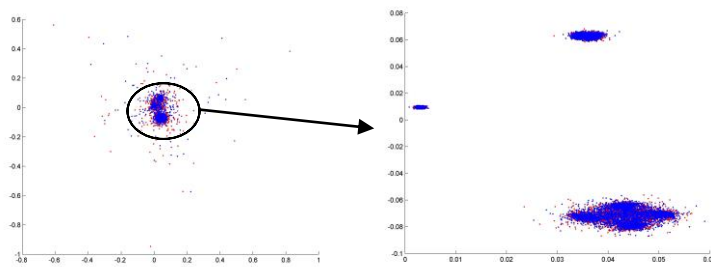
Fig. 18. The distributions of real values of the convergent sets for $a = 0.2$, $\theta = (75 * \pi / 180)$ and $degree = 3$ in the codomain.

5.2. Hierarchical Structures

The convergent sets in Fig. 16 have more internal structures as we examine in details. In the following, we study another set of parameters in equation (9) as below:

$$a = 0.1 (\cos(120 * \pi / 180) + \sin(120 * \pi / 180)) \text{ with } degree = 3 \text{ (9)}$$

The convergent sets in codomain as shown in Fig. 19(a) are further expanded in Fig. 19(b).



(a) Convergent sets in codomain (b) Expanded the circled area in (a)

Fig. 19. The distributions of the convergent sets for $a = 0.1$, $\theta = (120 * \pi / 180)$ and $degree = 3$ in the codomain.

We further expand the plot the three convergent groups of Fig. 19(b) to three individual plots as shown in Fig. 20. Then we select one of four sub-groups in Group 1 as shown Fig. 20(a), and expand one more level (2nd level) down to show the convergent sets as in Fig. 21.

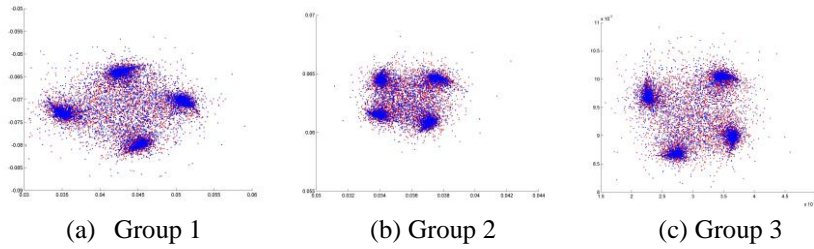


Fig. 20. The 1st-level expanded distributions of the convergent sets for $a = 0.1$, $\theta=(120*\pi/180)$ and $degree = 3$ in the codomain.

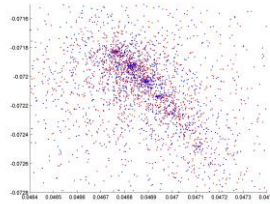


Fig. 21. The 2nd-level expanded distributions of the convergent sets for $a = 0.1$, $\theta=(120*\pi/180)$ and $degree = 3$ in the codomain.

Although we are studying in the momentum-angular-momentum space, we can still see the richness of this construction for modeling physical phenomena, such as formation of galaxy cluster and stellar system, statistics related to Boltzmann Equations and Navier-Stokes equation.

As an example of modeling the formation of our stellar system, we can adopt the momentum-angular-momentum groups shown in Fig. 21 to the formation of individual planets from flattening disk of the solar nebular system.

Conclusions

In this paper, we explore the chaotic transition based on the mathematical construction of the extended Blaschke product (EBP), which can be claimed as foundation of Nonlinear Relativity. We present the domain-codomain mapping

in the context of dynamical systems, and elaborate the convergent sets of solution to chaotic transition.

We can summarize our study as follows:

- The solution sets of chaotic transitions are discrete, simple, hierarchical, and slowly convergent in the momentum space comparing with those in temporal space.
- The solution sets of pre-chaos demonstrate discrete distributions and potentially provide models for formation and structure of galaxy cluster, Boltzmann Equation, Navier-Stokes equations, among other studies.
- The complex functions with conjugate forms produce root counts higher than that of FTA asserts.

We will further investigate this mathematical construction to the modeling of chaos in the future.

References

1. W. Blaschke, Eine Erweiterung des Satzes von Vitali, "über Folgen analytischer Funktionen" Berichte Math.-Phys. Kl., Sächs. Gesell. der Wiss. Leipzig, No. 67, pp. 194–200, 1915.
2. D. C. Ni and C. H. Chin, " $Z^{-1}C_1C_2C_3C_4$ System and Application", Proceedings of TIENCS workshop, Singapore, August 1-5, 2006.
3. D. C. Ni and C. H. Chin, Symmetry Broken in Low Dimensional N-body Chaos, Proc. of Chaos 2009 Conference, Chania, Crete, Greece, pp. 53 (Abstract), June 1-5, 2009.
4. D. C. Ni and C. H. Chin, Symmetry Broken in low dimensional N-Body Chaos, CHAOTIC SYSTEMS: Theory and Applications (ed. by C. H. Skidas and I. Domotikalis), pp. 215-223, 2010
5. D. C. Ni, "Chaotic Behavior Related to Potential Energy and Velocity in N-Body Systems", Proceedings of 8th AIMS International Conference on Dynamical Systems, Differential Equations and Applications, May 25-28, 2010, Dresden, Germany, pp. 328.
6. D. C. Ni and C. H. Chin, "Classification on Herman Rings of Extended Blaschke Equations", Differential Equations and Control processes, Issue No. 2, Article 1, 2010.
(<http://www.neva.ru/journal/j/EN/numbers/2010.2/issue.html>).
7. D. C. Ni, "Numerical Studies of Lorentz Transformation", Proceeding of 7th EASIAM, Kitakyushu, Japan, June 27-29, 2011, pp. 113-114.
8. D. C. Ni, "Statistics constructed from N-body systems", Proceeding of World Congress, Statistics and Probability, Istanbul, Turkey, July 9-14, 2012, pp. 171.
9. D. C. Ni, "Phase Transition Models based on A N-Body Complex Statistics", Proceedings of the World Congress on Engineering 2013 (WCE 2013), Vol I, pp. 319-323, July 3 - 5, 2013, London, U.K.
10. D.C. Ni, "A Counter Example of Fundamental Theorem of Algebra: Extended Blaschke Mapping", Proceedings of ICM 2014, August 13-August 21, Seoul, Korea, 2014.